

Classification of Individual Finger Movements from ECoG Signals using a Spiking Neural Network

Yulong Wang

Department of Electronic and Electrical Engineering
University College London, London, UK
yulong.wang.23@ucl.ac.uk

Sara Ghoreishizadeh

Department of Electronic and Electrical Engineering
University College London, London, UK
s.ghoreishizadeh@ucl.ac.uk

Abstract—We present the first classifier based on a spiking neural network (SNN) that can decode individual finger movements from electrocorticography (ECoG) signals. The SNN has only six leaky integrate-and-fire neurons and uses carefully selected features: the local motor potential and the high gamma band power to analyse a publicly available ECoG dataset. Through the investigation of the key aspects affecting SNN performance (epoch length, lag time, number of concatenated epochs), the presented decoder achieves a 72.4% average classification accuracy across three subjects with an average training time of 3.55 s and a latency of only 1 ms. This work demonstrates how a simple SNN architecture can effectively decode complex motor intentions from ECoG signals, potentially enabling more efficient brain-computer interfaces.

Index Terms—brain-computer interface (BCI), spiking neural network (SNN), motor decoding, electrocorticography (ECoG)

I. INTRODUCTION

Brain-computer interfaces (BCIs) can translate brain activity into actionable commands, allowing individuals to interact with their environments or control tailored devices, bypassing the biological neural pathways [1]. One of the most promising applications of BCIs lies in the development of motor neuroprostheses. These devices aim to restore motor functions in people suffering from paralysis due to spinal cord injuries, strokes, or neurodegenerative diseases [2].

Electroencephalography (EEG) is the most widely employed method for neural signal recording involved in motor decoding, due to its non-invasive nature. However, because EEG records neural activity directly from the scalp, it tends to perform poorly in decoding complex movement intentions. Intracortical recording instead provides high-fidelity measurements of local field potentials or single-unit/multi-unit activity, at the cost of high invasiveness because of the use of penetrating electrodes. In contrast, electrocorticography (ECoG) offers a balanced alternative by placing electrodes on the cortical surface.

There is increasing research on new brain implants capable of long-term ECoG recording and their application in motor decoding tasks [3], such as predicting lower limb movement to restore the ability of a patient with spinal cord injury to walk [4], and controlling an exoskeleton to perform reach-and-touch tasks and wrist rotations [5]. However, effective strategies for achieving dexterous hand control—especially individual finger movements—remain insufficiently explored. Achieving fast

and accurate individual finger movement decoding is crucial for patients with corresponding mobility impairment to regain the ability to perform daily tasks independently.

Different methods for individual finger movement decoding based on ECoG signals have been employed with up to 77% accuracy [6]. These methods range from traditional machine learning techniques such as conditional random fields (CRF) [7], support vector machines (SVM) and gradient boosting machines (GBM) [6] [8], to artificial neural networks (ANN) that consist of spatial and temporal convolutional layers [9]. However, the classification techniques demonstrated to date usually require complex models that demand significant computational resources, leading to high power consumption and latency issues.

To address these limitations, alternative classification methods based on spiking neural networks (SNNs) and neuromorphic computing have been proposed in other BCI applications [10] [11] [12]. SNNs more closely mimic biological neural networks by encoding information with discrete spikes. This approach contributes to reduced computational cost as SNNs reduce the dot-product operation in conventional ANNs to simple addition operation. Furthermore, the sparse nature of spike-encoded information allows for event-driven processing, reducing power consumption and data storage requirements [13]. Brain signal decoding using SNNs on neuromorphic hardware has been presented for successful classification of arm-reaching directions and detecting high-frequency oscillations associated with epilepsy onset [10] [11]. Although the superiority of SNNs for various BCI-related two-class and four-class classification tasks has been demonstrated [12], its use for more complex classification (six-class classification) required for individual finger movements decoding based on ECoG signals has not yet been investigated to the best of our knowledge. In this work, we demonstrate the feasibility of using a SNN to decode individual finger movements from ECoG signals. We show that a simple SNN can achieve comparable classification accuracy to that of the state-of-the-art, with significantly shorter training time and inference time.

II. METHODS

A. Dataset and Labelling

A publicly available dataset from the BCI competition IV was used in this study [14]. The dataset includes ECoG signals

recorded from three subjects while they performed self-paced finger movements in response to randomly displaced cues. The number of recording channels ranged from 48 to 64. The ECoG signals were recorded and amplified at a sampling frequency of 1000 Hz with instrumental bandpass filtering between 0.3 and 200 Hz. At the same time, individual finger trajectories were recorded at a sampling frequency of 25 Hz using a data-glove sensor (see Fig. 1a).

In this work, the recorded finger trajectories were individually re-labelled as binary events (with "0" representing the rest state and "1" representing finger movement) according to the method used in [6], where each complete movement period was considered a single movement state, without distinguishing multiple flexions within the period. After the movement state of each finger was determined, six classes were labelled from "0" to "5", with "0" representing the rest state, and "1" to "5" representing the movement of the thumb to little fingers.

B. Sample Construction and Feature Selection

The recorded ECoG signals of each channel were re-referenced to the common average of all channels to reduce common noise. Local motor potential (LMP, running average of the raw signal [14]) and power in different frequency bands were then computed for each channel and normalized to fit within 0 to 1. The band powers were calculated across five spectral bands: alpha band (8 to 13 Hz), beta band (13 to 30 Hz), low gamma band (30 to 55 Hz), and high gamma band (HGB) from both 65 to 115 Hz and 125 to 175 Hz (referred to as HG1 and HG2 from now on). The three gamma bands were divided in this manner to avoid the use of notch filters to eliminate power-line interference at 60 Hz and its harmonics. Both LMP and the five band powers were calculated based on the running average over a specified epoch length, with a fixed step size of 40 ms to align with the sampling frequency of the finger trajectories (Fig. 1b). Furthermore, historical data were concatenated by introducing an additional dimension when constructing the samples before passing the data into the SNN model (Fig. 1c).

To identify the most informative features among the aforementioned six feature types, squared Pearson's correlation coefficient (r^2) was calculated between each feature and the preprocessed finger trajectories (with baseline drift reduction and resting noise removal). The five finger trajectories were also combined as one to form a new category for r^2 evaluation, aiming to determine which features could exhibit the highest correlation with finger movements in general, regardless of which specific finger was moving.

C. Temporal Dynamics Analysis

The execution of finger movements is known to be correlated with ECoG signals recorded several hundred milliseconds ago [15]. To study the impact on the performance of the classifier by extracting the temporal features differently, the following aspects were investigated: the epoch length of the selected features, the lag time between the samples and the labels, and the number of concatenated epochs. The epoch

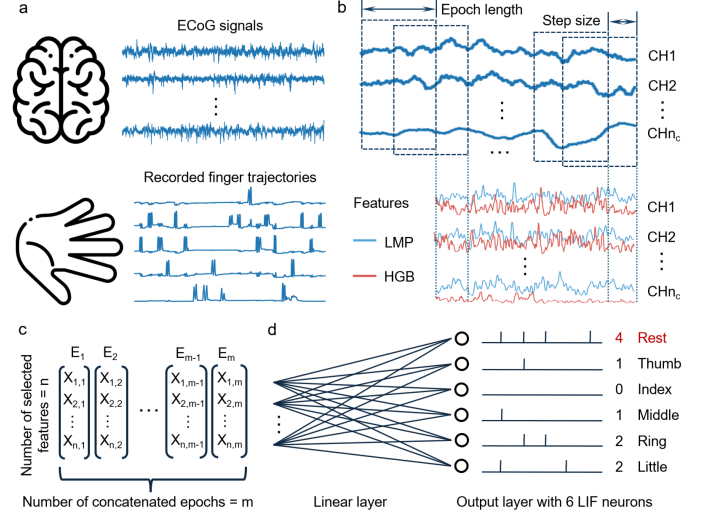


Fig. 1. **a.** Examples of the raw ECoG signal and individual finger trajectories provided in the BCI competition IV dataset. **b.** The features computed based on the specified epoch length and step size, containing LMP and power of different frequency bands (only LMP and high gamma band power (HGB) from 65 to 115 Hz are shown here as an example). **c.** Each sample that was to be passed into the neural network contained n selected features, with m concatenated epochs. **d.** These samples were fed to the output layers through a linear layer. The output layer consisted of 6 LIF neurons that corresponded to the 6 classes to be predicted. The predicted class was determined by the neuron that spiked the most. In this example, the predicted class is the class that corresponds to the rest state.

length was varied from 200 to 2000 ms, while lag times from 0 to 400 ms were applied. The impact of using different numbers of concatenated epochs on the model performance was examined from the number of 1 (no concatenation) to 26 (concatenation with the previous 25 epochs) for different epoch lengths.

D. Spiking Neural Network Model and Training

We employed a simple SNN as the classifier where the input features were directly connected to six output spiking neurons, corresponding to the rest class and the five movement classes, through a fully connected linear layer as shown in Fig. 1d. The spiking neuron model used was the leaky integrate-and-fire (LIF) model without a refractory period as described in [16]. This simplified LIF model involved only two hyperparameters: the membrane potential decay constant and the threshold potential, both of which were uniformly applied to the six spiking neurons.

The SNN model was trained using surrogate gradient descent that replaces the non-differentiable step function describing the spiking behaviour with the arctangent function [17]. As each sample contained input from multiple time steps, backpropagation through time (BPTT) was used for training based on the sum of the loss from each time step as proposed in [18]. The class corresponding to the output neuron with the maximum spike count over the time steps was considered the predicted class (Fig. 1d).

To achieve the optimal model performance, the epoch length, the lag time, the number of concatenated epochs,

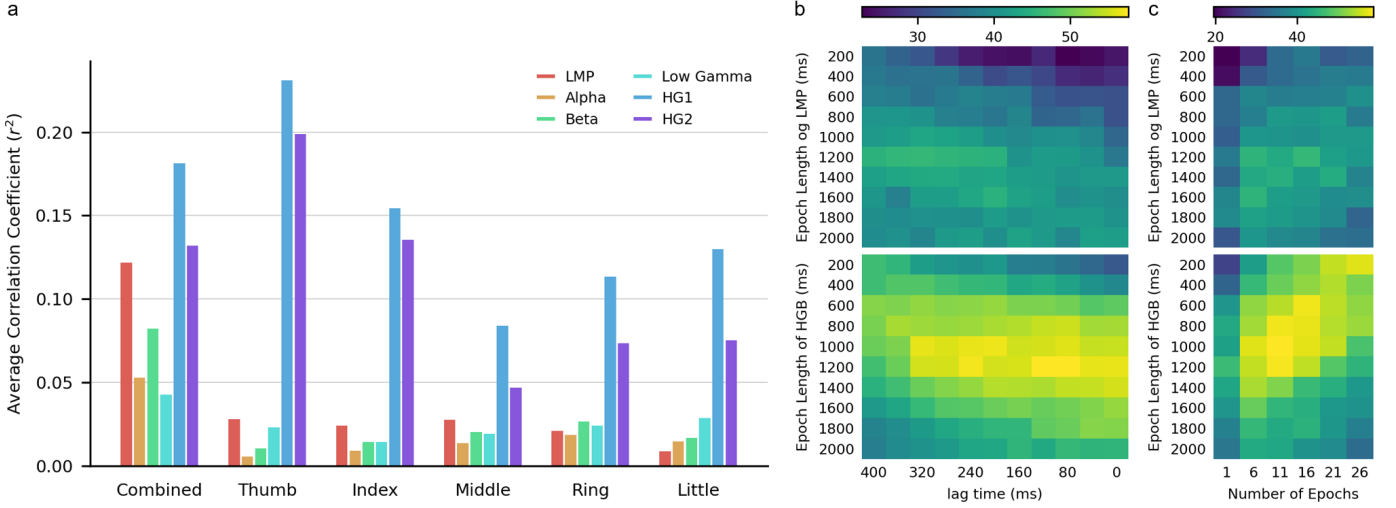


Fig. 2. **a.** The average correlation coefficients of the highest value achieved among all channels between each feature type and each finger movement category for the three subjects. A uniform epoch length of 200 ms and a zero lag time were used in this plot. **b.** Classification accuracy of the trained models using features computed from different epoch lengths and lag times (with 6 concatenated epochs). **c.** Classification accuracy obtained using different epoch lengths and numbers of epochs concatenated to construct the samples (with a zero lag time). Both **b** and **c** are from the results of subject 2, where the upper ones used LMP alone as input features and the lower ones used HGB (HG1 for subject 2).

and the number of included features were optimized for each subject. In particular, the epoch lengths were applied differently for different types of features selected. And they were treated as the hyperparameters together with the lag time. With the feature types to be used determined during feature selection, instead of using all channels, the optimal number of features that minimize the model's complexity while maintaining high performance was to be determined. This was done by adding the features one by one in the order of their correlation coefficients (highest correlation first) with the specific finger trajectories to check the performance of the trained SNN until no significant improvement in the classification accuracy observed. The SNN model was trained and run on an NVIDIA GeForce RTX 4080 GPU. And during the training process, five-fold cross-validation was employed for hyperparameter tuning and model performance evaluation.

III. RESULTS AND DISCUSSION

A. Feature Selection

The highest correlation achieved between each feature type and the finger movement category is plotted in Fig. 2a, where each bar represents the average of three correlation coefficients obtained from the three subjects. It can be observed that the LMP primarily correlates with combined finger trajectories. And spectral features, particularly the HGB powers (both HG1 and HG2) provide more insights into individual finger movements. As HG1 and HG2 highly correlate with each other (with an average correlation coefficient of 0.378 across all channels and subjects), only the one with the highest correlation was selected for each subject. That was HG1 for subjects 2 and 3, and HG2 for subject 1.

B. Epoch Length and Lag Time

Fig. 2b shows the accuracy of the models trained by using different epoch lengths for LMP and HGB (HG1 for subject 2), with different lag times for subject 2. It can be observed that using LMP alone with no additional delay (beyond the inherent recording lag, 37 ± 3 ms according to [14]), the maximum accuracy of 42.2% is obtained at an epoch length of 2000 ms. While a 200 ms epoch length, as adopted in [6], can only achieve an accuracy of 24.8% at a zero lag time. This suggests that the optimal lag time correlates with the specific epoch length used. A similar pattern is observed for HGB, where using relatively longer epoch lengths coupled with shorter lag times leads to higher classification accuracy.

C. Epoch Length and Concatenation

As shown in Fig. 2c, compared with applying no concatenation, using only six concatenated epochs can effectively improve the classification accuracy for subject 2. And this improved the accuracy by 3.9% for LMP and 10.2% for HGB across different epoch lengths and subjects on average. Using shorter epoch lengths, typically requires concatenating more epochs to enhance accuracy. However, there is a trade-off between the selection of epoch length and concatenation number—longer epoch lengths increase preprocessing demands, while a larger number of concatenated epochs means passing through the SNN more times, which increases the computational load and introduces additional latency.

D. Model Optimization

To simplify the training process, uniform lag time and number of concatenated epochs were applied to both LMP and HGB (HG1 or HG2 depending on the subject) features. Though using more concatenated epochs to construct the samples can sometimes contribute to higher classification

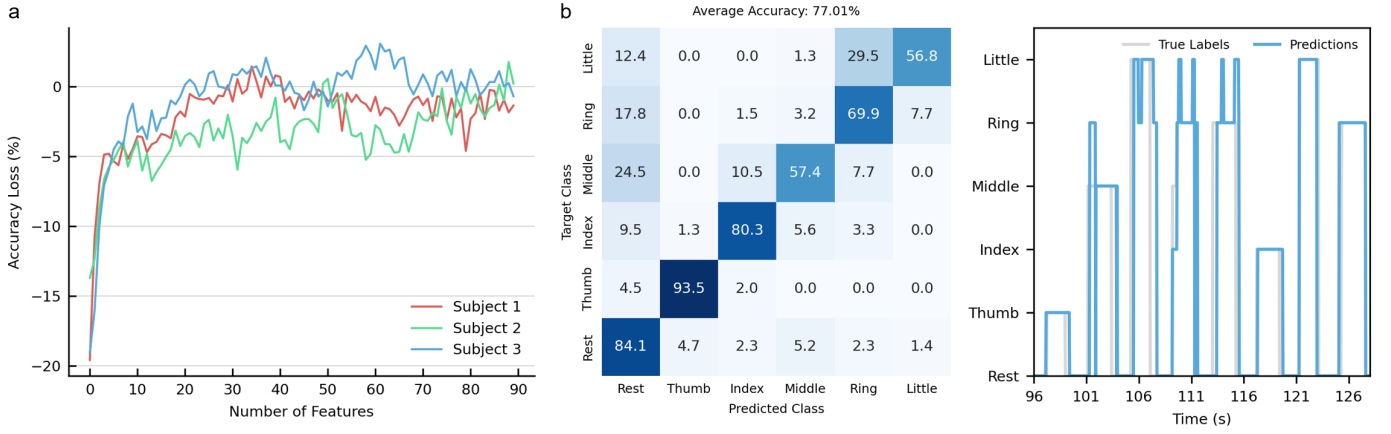


Fig. 3. **a.** Accuracy loss of the classification models from the 3 subjects with different numbers of features used for training. **b.** Confusion matrix showing the detailed classification accuracy achieved for subject 3. A segment of the test labels from BCI competition IV dataset and the predictions made by the SNN model are shown on the right.

TABLE I
OPTIMIZED HYPERPARAMETERS AND THE FINAL CLASSIFICATION ACCURACY FOR THE THREE SUBJECTS

Subject	Epoch Length <i>LMP</i>	Epoch Length <i>HGB</i>	Lag Time	No. of Epochs	No. of Features	ACC (%)
1	1400	1200	120	6	40	65.73
2	400	1000	200	6	40	74.35
3	1400	600	80	6	38	77.01

Epoch length and lag time are in milliseconds.

TABLE II
CLASSIFICATION ACCURACY FROM PREVIOUS WORK AND THE PROPOSED SNN MODEL

Reference	Model	Training Time (s)	Inference Time (s)	ACC (%)
Jaime'16 [7]	CRF	—	—	65.3
Guillaume'19 [9]	ANN	—	—	64.2
Lin'22 [6]	SVM-rbf	26.1	14.7	76.0
Lin'22 [6]	lightGBM	17.2	0.02	77.0
This work	SNN	3.55	0.001	72.4

accuracy, considering hardware limitations as described in III-C, the number of concatenated epochs was fixed at six. After determining the optimal epoch lengths of LMP and HGB, and the lag time for the three subjects, the accuracy loss by including different numbers of features is shown in Fig. 3a. Notably, limiting the number of features to an optimal amount can lead to a higher accuracy than including all available features (LMP and HGB from all channels). Specifically, with computational cost considered, subject 1 achieved the optimal performance with a classification accuracy of 66% with 40 features (27 LMP and 13 HGB features); subject 2 reached 74% accuracy with 40 features as well (25 LMP and 15 HGB features); and subject 3 obtained 77% accuracy with 38 features (23 LMP and 15 HGB features) as shown in Fig. 3b. A summary of the optimized hyperparameters is listed in Table I.

The average training time and inference time of the optimized SNN model were found to be 3.55 s and 1.0 ms respectively. Further improvement in inference time is anticipated when implementing the model on dedicated neuromorphic hardware. A comparison with previous classification methods based on the same dataset shows that the average classification accuracy of 72.4% achieved in this work outperforms the prior works based on the CRF model and the ANN model (Table II). Although higher accuracy has been achieved using the modified SVM and GBM methods [6], both the training time and the inference time of these methods are substantially longer than what we achieved in this work.

IV. CONCLUSION

A simple SNN with six LIF neurons is presented to decode individual finger movements from ECoG signals. Based on the correlation coefficients between different types of features and the finger trajectories, LMP and HGB were identified as the most informative feature types and selected as the input features for the SNN model. It was observed that employing longer epoch lengths allowed for the use of fewer successive epochs concatenated to achieve a higher classification accuracy. And using a subset of features that exhibited higher correlation was also found to have a better performance than including the entire feature set. Overall, the proposed model achieved real-time inference with an average classification accuracy of 72.4% across three subjects. The achieved accuracy is comparable to that of the state-of-the-art approach [6], while with an order of magnitude shorter in training time and inference time.

REFERENCES

- [1] J. R. Wolpaw, N. Birbaumer, D. J. McFarland, G. Pfurtscheller, and T. M. Vaughan, "Brain-computer interfaces for communication and control," *Clinical Neurophysiology*, vol. 113, no. 6, pp. 767–791, Jun. 2002.
- [2] M. Chiappalone et al., "Neuromorphic-Based Neuroprostheses for Brain Rewiring: State-of-the-Art and Perspectives in Neuroengineering," *Brain Sciences*, vol. 12, no. 11, pp. 1578, Nov. 2022.
- [3] K. M. Szostak, L. Grand, and T. G. Constantinou, "Neural Interfaces for Intracortical Recording: Requirements, Fabrication Methods, and Characteristics," *Frontiers in Neuroscience*, vol. 11, Dec. 2017.

- [4] H. Lorach et al., "Walking naturally after spinal cord injury using a brain–spine interface," *Nature*, vol. 618, pp. 1–8, May 2023.
- [5] A. L. Benabid et al., "An exoskeleton controlled by an epidural wireless brain-machine interface in a tetraplegic patient: a proof-of-concept demonstration," *The Lancet Neurology*, vol. 18, no. 12, Oct. 2019.
- [6] L. Yao, B. Zhu, and M. Shoaran, "Fast and accurate decoding of finger movements from ECoG through Riemannian features and modern machine learning techniques," *Journal of Neural Engineering*, vol. 19, no. 016037, Jan. 2022.
- [7] J. F. Delgado Saa, A. de Pestere, and M. Cetin, "Asynchronous decoding of finger movements from ECoG signals using long-range dependencies conditional random fields," *Journal of Neural Engineering*, vol. 13, no. 3, p. 036017, May 2016.
- [8] L. Yao and M. Shoaran, "Enhanced Classification of Individual Finger Movements with ECoG," 2019 53rd Asilomar Conference on Signals, Systems, and Computers, Nov. 2019.
- [9] G. Jubien, M.-C. Schaeffer, S. Bonnet, and Tetiana Aksenova, "Decoding of finger activation from ECoG data: a comparative study," 2019 International Joint Conference on Neural Networks (IJCNN), Budapest, Hungary, Jul. 2019.
- [10] I.-A. Lungu, A. Riehle, M. P. Nawrot, and M. Schmuker, "Predicting voluntary movements from motor cortical activity with neuromorphic hardware," *IBM journal of research and development*, vol. 61, no. 2/3, pp. 5:1–5:12, Mar. 2017.
- [11] M. Sharifshazileh, K. Burelo, J. Sarnthein, and G. Indiveri, "An electronic neuromorphic system for real-time detection of high frequency oscillations (HFO) in intracranial EEG," *Nature Communications*, vol. 12, no. 1, May 2021.
- [12] N. Kumar, G. Tang, R. Yoo, and K. P. Michmizos, "Decoding EEG With Spiking Neural Networks on Neuromorphic Hardware," *Transactions on Machine Learning Research*, Jun. 2022.
- [13] K. Roy, A. Jaiswal, and P. Panda, "Towards spike-based machine intelligence with neuromorphic computing," *Nature*, vol. 575, no. 7784, pp. 607–617, Nov. 2019.
- [14] G. Schalk et al., "Decoding two-dimensional movement trajectories using electrocorticographic signals in humans," *Journal of Neural Engineering*, vol. 4, no. 3, pp. 264–275, Jun. 2007.
- [15] S. Acharya, M. S. Fifer, H. L. Benz, N. E. Crone, and N. V. Thakor, "Electrocorticographic amplitude predicts finger positions during slow grasping motions of the hand," *Journal of Neural Engineering*, vol. 7, no. 4, p. 046002, May 2010.
- [16] J. K. Eshraghian et al., "Training Spiking Neural Networks Using Lessons From Deep Learning," *Proceedings of the IEEE*, vol. 111, no. 9, pp. 1016–1054, Sep. 2023.
- [17] E. O. Neftci, H. Mostafa, and F. Zenke, "Surrogate Gradient Learning in Spiking Neural Networks: Bringing the Power of Gradient-Based Optimization to Spiking Neural Networks," *IEEE Signal Processing Magazine*, vol. 36, no. 6, pp. 51–63, Nov. 2019.
- [18] P. J. Werbos, "Backpropagation through time: what it does and how to do it," *Proceedings of the IEEE*, vol. 78, no. 10, pp. 1550–1560, 1990.